

Supporting Information for:
Mispacking of the Phe87 side chain reduces the kinetic stability of human transthyretin

Xun Sun, Marcus Jaeger, Jeffery W. Kelly, H. Jane Dyson, Peter E. Wright*

Affiliations:

Department of Integrative Structural and Computational Biology, Department of Chemistry, and Skaggs Institute of Chemical Biology, The Scripps Research Institute, 10550 North Torrey Pines Road, La Jolla, CA 92037, U.S.

* Correspondence to Peter E. Wright wright@scripps.edu

Materials and Methods

Protein expression, purification and labeling

The following primers were used to generate designated mutations:

S10A_f: 5'-ctttgaccatcagaggagccttgattcaccggtgc-3'

S10A_r: 5'-gcaccggatgaatccaaggctcctctgatggtaaag-3'

S46C_f: 5'-tggttttccacaggcaaatggctcccagg-3'

S46C_r: 5'-cctgggagccatttgcctgtgggaaaacca-3'

E63C_f: 5'-ctttgtatatccctctacaaagcactcctcagttgtgagcccatgc-3'

E63C_r: 5'-gcattgggctcacaactgaggagtgctttgtagaaggatatacaaag-3'

Mutagenesis was performed according to the manufacturers' instruction for the QuikChange kit (Agilent). Protein expression, purification and labeling was carried out as previously reported.¹ An extinction coefficient of $18,450 \text{ M}^{-1}\text{cm}^{-1}$ was used to calculate the monomer concentration of TTR, which was reported throughout this work. C10S-S85C was chosen over C10A-S85C as the protein template for ^{19}F -NMR study because of the higher yield of the former construct.

^{19}F -NMR experiments

All ^{19}F -NMR experiments were performed on a Bruker Avance 601 spectrometer with a QCI cryoprobe and a shielded z-gradient coil. Typically, a 90° pulse (10–12 μs) was used and the recycling delay was set to 1 s. Each spectrum was acquired with 4k complex points. A line broadening factor of 1 Hz was used prior to zero filling to 16k points. The apodization, zero-filling and Fourier transformation were performed using NMRPipe.² Unless otherwise noted, the buffer used was either 10 mM potassium phosphate with 100 mM potassium chloride at pH 7.0 (GF buffer) or 50 mM sodium acetate with 100 mM potassium chloride at pH 4.4 (aggregation buffer).

The relative translational diffusion coefficient of the major (T) and minor (T*) conformations was measured by a ^{19}F longitudinal encode-decode diffusion-ordered NMR experiment (^{19}F -DOSY) as previously described.^{1, 3} Ten evenly spaced relative z-gradient strengths from 5% to 50% were used in the measurement (Figure 1D). Each experiment was scanned for 2k times in an interleaved manner and the total time of experiment was 7.5 h.

For the T-T* exchange experiment, A120L in GF buffer was added to TTR^{F} in the same buffer so that the final monomer concentration was 10 μM for TTR^{F} and 80 μM for A120L. The high molar ratio of A120L to TTR^{F} was used to enhance the population of T*. A correction was made for the mixing dead time of 23 mins so that time zero corresponds to the time when the two solutions were manually mixed (Figure 2A). The interconversion of T and T* conformations enabled by the TTR^{F} subunit exchange was monitored at pH 7.0 and 298 K for a time course of 66 h. Each experiment was recorded for 3 h and normalized by the total peak area. The time-dependent changes in the intensity of the ^{19}F resonances of T and T* were fitted with a Lorentzian line shape and the relative peak areas were used to extract the exchange kinetics by a single exponential function (Figure 2C). In this mixing experiment, the rate limiting step is the dissociation of TTR^{F} . The subunit exchange for A120L is expected to be faster than that of TTR^{F} so that it was not measurable here.

The ^{19}F T_2 measurement for T and T* of TTR^{F} premixed with 8-fold A120L in GF buffer at 298 K for 3 d was performed using a Carr–Purcell–Meiboom–Gill (CPMG) pulse sequence.⁴ Nine sets

of 180° ^{19}F pulses (2, 4, 8, 16, 32, 64, 128, 256 and 512) were applied and the delay between two 180° pulses was set to be 250 μs . The recycling delay was set to be 2 s. The measured T_2 is 35 ± 2 ms for T and 24 ± 2 ms for T* at pH 7.0 and 298 K. The uncertainty in T_2 was calculated as one standard deviation from 50 bootstrapped datasets. The ^{19}F T_1 measurement was performed using an inversion recovery pulse program as previously described.¹ The measured T_1 is 0.36 ± 0.04 s for T and 0.40 ± 0.07 s for T* in the same premixed sample. Since the T_1 is very similar for T and T*, no T_1 correction of peak area was performed for the peak area quantification.

Direct quantification of the tetramer and the monomer populations of C10S-S85C-A120L-BTFA using ^{19}F -NMR was not possible as the labeled protein aggregates at the high concentrations that are necessary for tetramerization. To determine the oligomerization state of A120L, we performed ^{15}N -filtered DOSY experiments to measure the translational diffusion coefficient (D) of ^{15}N -labeled A120L in GF buffer at 298 K on a Bruker Avance 900 spectrometer equipped with a TXI probe. The Stejskal–Tanner equation⁵ was used to extract D from 11 diffusion-ordered transients. D is $(5.0 \pm 0.1) \times 10^{-7}$ cm^2/s for A120L at 800 μM and it increases to $(6.3 \pm 0.2) \times 10^{-7}$ cm^2/s at 100 μM , which is comparable to D of $(5.9 \pm 0.2) \times 10^{-7}$ cm^2/s for F87A at 100 μM and D of $(6.1 \pm 0.2) \times 10^{-7}$ cm^2/s for F87M at 60 μM . For reference, D is $(5.1 \pm 0.2) \times 10^{-7}$ cm^2/s for the WT TTR tetramer at 100 μM ⁶ and is $(7.6 \pm 0.1) \times 10^{-7}$ cm^2/s for a monomeric F87E mutant at 100 μM . Given that both F87A and F87M are mixtures of tetramer and monomer (Figure S1 and Ref⁷), this comparison suggests that A120L at 100 μM is also a mixture of tetramer and monomer. To rule out the contribution of the tetramer-monomer exchange on D ,⁸ we measured the exchange between the tetramer and the monomer of F87A^F at pH 7.0 and 298 K to be ~ 0.8 h^{-1} by the real-time ^{19}F -NMR temperature alternation from 277 K to 298 K. Therefore, the slow exchange kinetics between the tetramer and the monomer is unlikely to contribute to the concentration-dependent D changes in TTR mutants. Accordingly, D of 6.3×10^{-7} cm^2/s of 100 μM A120L likely represents a mixture of tetramer and monomer without exchange on the DOSY timescale (200 ms in our measurements).

For the urea-unfolding experiment at 298 K, a solution of 6 M urea, 55 mM potassium phosphate, 100 mM KCl, 0.5 mM disodium EDTA and 5 mM dithiothreitol at pH 7.0 was used. For unfolding of TTR^F without A120L, the mixing dead time was 10 mins. The predicted unfolding rate (0.067 h^{-1}) equals $\exp(\log(0.038) + 0.094 \times 6)$, where the dissociation rate of TTR^F without urea (0.038 h^{-1}) is from Figure 2C, the urea-dependent unfolding rate coefficient for WT TTR (0.094 M^{-1}) is from Ref⁹ and the urea concentration is 6 M. The mixing dead time was 17 mins for the urea-unfolding experiment for 10 μM TTR^F premixed with 8-fold A120L, which was incubated at 298 K and pH 7.0 for 3 d. Based on the conservation of the ^{19}F -NMR signal, we normalized the spectra before and after the addition of urea using total peak areas and rescaled all spectra so that the peak intensity of T before urea mixing equals 1 (Figure 3A). The peak areas of the residual T and the unfolded U conformations in each spectrum were fitted by two Lorentzian functions and follow the same kinetics (0.26 ± 0.02 h^{-1}).

For the ^{19}F -NMR aggregation assay, the pre-mixed A120L:TTR^F (8:1) solution in GF buffer was mixed with $3 \times (\text{vol/vol})$ aggregation buffer to initiate aggregation at 298 K. The mixing dead time was 10 mins and each spectrum was recorded for 1 h with a total acquisition time of 65 h. For illustrative purposes, a double exponential function was used to fit the peak intensity for the residual T resonance to allow intensity extrapolation at time zero when the pH was lowered from

7.0 to 4.4. The three-state aggregation kinetics ($T \xrightleftharpoons[k_{-1}]{k_1} I \xrightleftharpoons[k_{-2}]{k_2} A$) was fitted as previously described for the premixed sample.¹ All the data points for each T, I and A species were used, but only one out of three data points was plotted for clarity (Figure 3D). The root-mean-square error of the fitting is 0.033 in the normalized peak area.

Table S1 Concentration-independence of the relative population of T* in TTR^F

Concentration ^a	T* (%) ^b
360 μ M	5.4
130 μ M	8.0
40 μ M	7.9
10 μ M	6.0

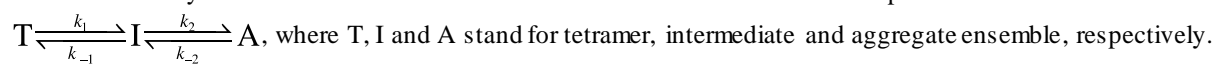
^a The monomeric TTR concentration is reported and the measurements were performed for four samples from four independently expressed and labeled protein batches in GF buffer at 298 K.

^b The fitted Lorentzian peak areas of T* relative to the sum of the fitted peak areas of T and T*.

Table S2 Aggregation kinetics for TTR^F with and without A120L at pH 4.4 and 298 K

Condition	k_1 (h ⁻¹) ^a	k_{-1} (h ⁻¹) ^a	k_2 (h ⁻¹) ^a	k_{-2} (h ⁻¹) ^a
10 μ M TTR ^F ^b	0.13 \pm 0.02	0.63 \pm 0.10	0.06 \pm 0.01	0.01 \pm 0.01
10 μ M TTR ^F + 80 μ M A120L	1.51 \pm 0.47	7.85 \pm 2.10	0.99 \pm 0.33	0.03 \pm 0.01

^a The uncertainty was calculated as one standard deviation from 50 bootstrap datasets. The kinetic model is



^b Fitted parameters for TTR^F are from Ref¹.

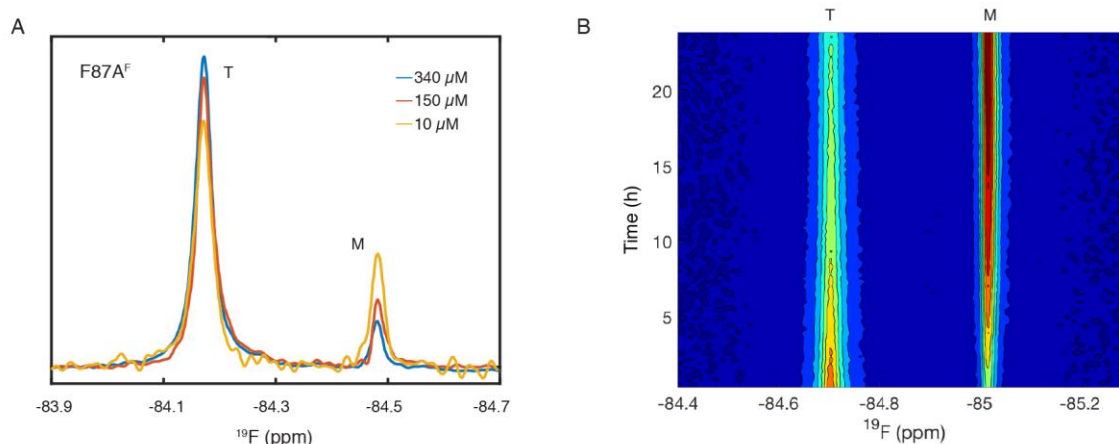


Figure S1. Enhancing the population of monomer (M) at the cost of tetramer (T) in F87A^F by dilution at pH 7.0 and 298 K (A) and by reducing temperature from 298 K to 277 K at pH 7.0 (B). The peak areas in (A) are normalized for comparison. Reducing the temperature causes 0.53–0.54 ppm upfield shifts of the ^{19}F chemical shifts for both peaks. The time resolution of the intensity contour in (B) is 1 h. The relative intensity from high to low is colored from red to blue.

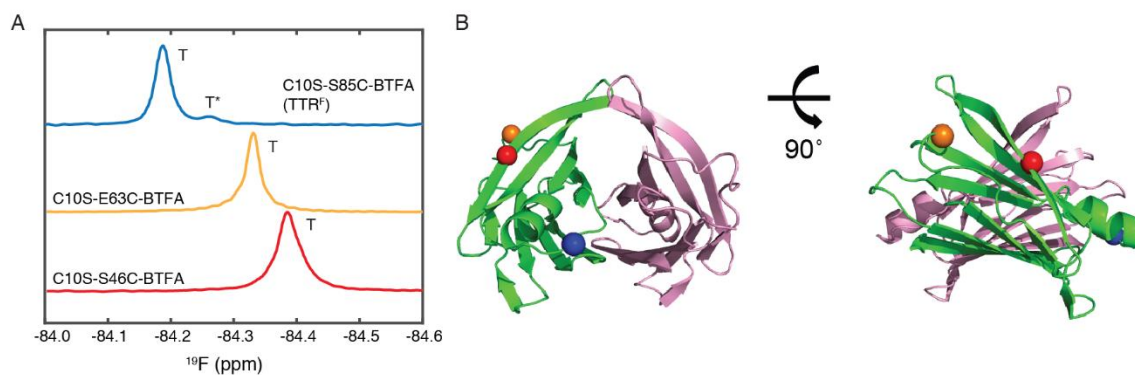


Figure S2. ^{19}F -NMR spectra and labeling sites of TTR^{F} (C10S-S85C-BTFA), C10S-E63C-BTFA and C10S-S46C-BTFA. (A) The main ^{19}F tetramer resonances (T) of E63C-BTFA and S46C-BTFA do not show the upfield minor conformation (T^*) at pH 7.0/298 K. (B) The BTFA labeling sites of S85 (blue), E63 (orange) and S46 (red) with $\text{C}\alpha$ shown as spheres. Two protomers in one strong dimer pair in WT TTR (PDB: 1BMZ)¹⁰ are colored in green and pink, respectively.

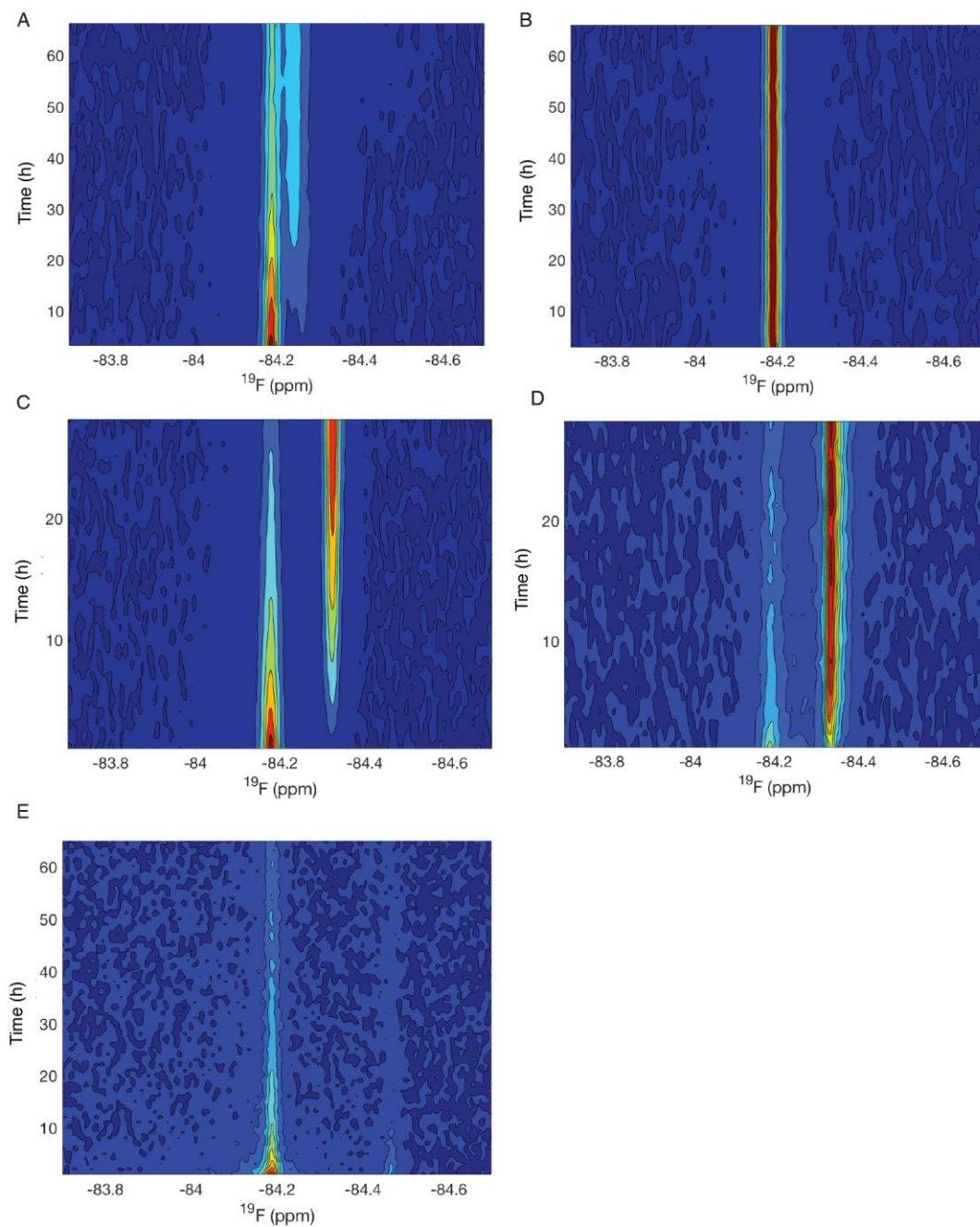


Figure S3. (A) Time dependent changes in the ^{19}F NMR spectrum of TTR^{F} mixed with 8-fold A120L at pH 7.0 and 298 K. (B) TTR^{F} alone at pH 7.0 and 298 K. (C) TTR^{F} unfolded by 6 M urea at pH 7.0 and 298 K. (D) TTR^{F} pre-incubated with 8-fold A120L at pH 7.0 and 298 K and then unfolded by 6 M urea. (E) TTR^{F} pre-incubated with 8-fold A120L at pH 7.0 and 298 K and then aggregated at pH 4.4 and 298 K.

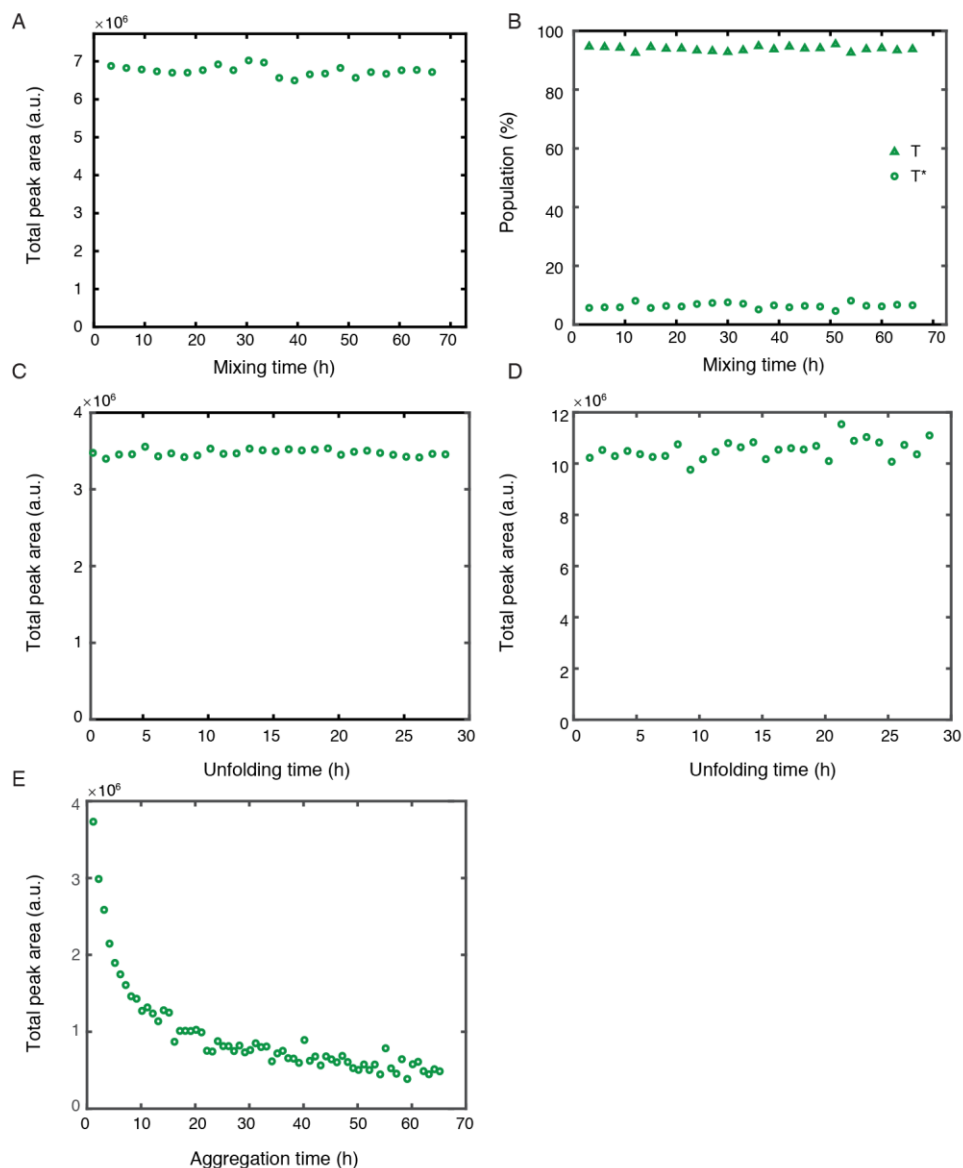


Figure S4. (A) Total peak areas of the two conformations ($T+T^*$) remain constant for TTR^F mixed with 8-fold of A120L for 66 h at pH 7.0 and 298 K. (B) Relative populations of T and T^* are constant for TTR^F alone at pH 7.0 and 298 K for the observation time of 66 h. (C) Total peak areas of T and unfolded (U) in TTR^F are constant in the presence of 6 M urea at pH 7.0 and 298 K. (D) Invariant total peak areas of T and U of TTR^F pre-incubated with 8-fold A120L and then unfolded by 6 M urea at pH 7.0 and 298 K. (E) Total peak areas of T and I decay over time for TTR^F premixed with 8-fold A120L at pH 7.0 and 298 K and then aggregated at pH 4.4 and 298 K.




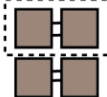

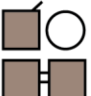
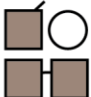

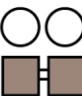

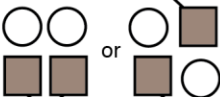


Legend:	Possible mixed species	^{19}F resonance	Number of correctly packed dimer pairs
 TTR protomer (with BTFA at S85C)			
 F87 side chain			
 A120L protomer (without BTFA at S85C)			
 X: unmixed T in TTR^{F} (two pairs of correctly packed dimers)			
 Y: unmixed T^* in TTR^{F} (one pair of correctly packed dimers)			
	A 	T + T^*	1
	B 	T + T^*	0
	C 	T^*	0
	D 	T	1
	E 	T + T^*	0
	F  or 	T^*	0
	G 	T^*	0

Figure S5. Cartoon showing possible species in the A120L: TTR^{F} mixture prior to urea unfolding. The strong dimer interface is shown as a dashed box in the species X. Steric clash due to incorporation of A120L into a dimer pair would force out the side chain of F87 to generate the T^* conformation in the other protomer, leading to the loss of one correctly packed dimer pair. Due to pre-incubation with a large excess of A120L (8:1 monomer mole ratio for A120L: TTR^{F}), the population of T and T^* species containing no A120L (species X and Y) and of heterotetramers containing only one A120L protomer (species A, B and C) is expected to be very small. The near complete loss of the T^* resonance within 1 h ($k_{\text{obs}} > 1 \text{ h}^{-1}$) and the much slower decay of T (0.26 h^{-1}) following addition of urea (Figure 3A) suggests that the population of species with co-existing T and T^* states (species A, B and E) is also very small; for such species, the T and T^* decay rates would be identical. It is therefore likely that, under our experimental conditions, the heterodimer D is the major species associated with the T resonance while heterodimers F and G give rise to the T^* resonance (Figure 3A).

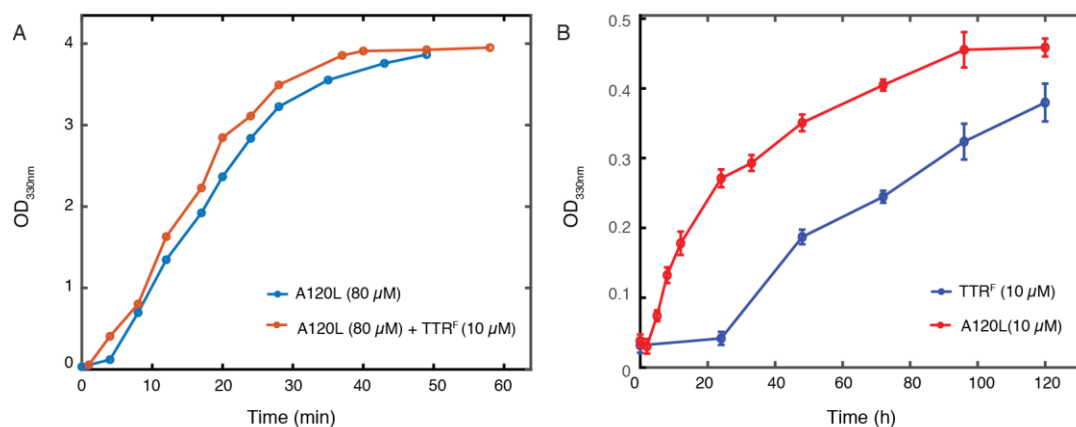


Figure S6. (A) The optical density at 330 nm (OD_{330nm}) for A120L (80 μM) and A120L (80 μM) with TTR^F (10 μM) at pH 4.4 and 298 K. A120L was premixed with TTR^F at pH 7.0 and 298 K for 2 days before lowering the pH to 4.4, in a way similar to the ¹⁹F-NMR aggregation experiment (Figure 3C). (B) OD_{330nm} for A120L (10 μM) and TTR^F (10 μM) at pH 4.4 and 298K. Error bars in (B) denote one standard deviation from three independent measurements.

Reference:

- (1) Sun, X., Dyson, H. J., and Wright, P. E. (2018) Kinetic analysis of the multi-step aggregation pathway of human transthyretin, *Proc. Natl. Acad. Sci. U.S.A.* 115, E6201–E6208.
- (2) Delaglio, F., Grzesiek, S., Vuister, G. W., Zhu, G., Pfeifer, J., and Bax, A. (1995) NMRPipe: A multidimensional spectral processing system based on UNIX pipes, *J. Biomol. NMR* 6, 277–293.
- (3) Altieri, A. S., Hinton, D. P., and Byrd, R. A. (1995) Association of biomolecular systems via pulsed field gradient NMR self-diffusion measurements, *J. Am. Chem. Soc.* 117, 7566–7567.
- (4) Meiboom, S., and Gill, D. (1958) Modified spin - echo method for measuring nuclear relaxation times, *Rev. Sci. Instrum.* 29, 688 – 691.
- (5) Stejskal, E. O., and Tanner, J. E. (1965) Spin diffusion measurements: Spin echoes in the presence of a time-dependent field gradient, *J. Chem. Phys.* 42, 288–292.
- (6) Sun, X., Dyson, H. J., and Wright, P. E. (2017) Fluorotryptophan incorporation modulates the structure and stability of transthyretin in a site-specific manner, *Biochemistry* 56, 5570–5581.
- (7) Jiang, X., Smith, C. S., Petrassi, H. M., Hammarstrom, P., White, J. T., Sacchettini, J. C., and Kelly, J. W. (2001) An engineered transthyretin monomer that is nonamyloidogenic, unless it is partially denatured, *Biochemistry* 40, 11442–11452.
- (8) Johnson, C. S. (1999) Diffusion ordered nuclear magnetic resonance spectroscopy: principles and applications, *Prog. Nucl. Magn. Reson. Spectrosc.* 34, 203–256.
- (9) Hammarstrom, P., Jiang, X., Hurshman, A. R., Powers, E. T., and Kelly, J. W. (2002) Sequence-dependent denaturation energetics: A major determinant in amyloid disease diversity, *Proc. Natl. Acad. Sci. U.S.A.* 99 (Suppl. 4), 16427–16432.
- (10) Peterson, S. A., Klabunde, T., Lashuel, H. A., Purkey, H., Sacchettini, J. C., and Kelly, J. W. (1998) Inhibiting transthyretin conformational changes that lead to amyloid fibril formation, *Proc. Natl. Acad. Sci. U.S.A.* 95, 12956–12960.